Proceedings of the Seventh International Conference on
Railway Technology: Research, Development and Maintenance
Edited by: J. Pombo
Civil-Comp Conferences, Volume 15, Paper 16.2
Civil-Comp Press, Edinburgh, United Kingdom, 2026
ISSN: 2753-3239, doi: 10.4203/ccc.15.16.2

Development and Validation of a Numerical Track Model with Resilient Layers for Heavy Haul Railways

A. Shamohammadi[1], E. Kassa[2], A. Bouazza[1], T. Marolt Čebašek[3] and C. Qiu[2]

[1]Department of Civil and Environmental Engineering (CEE), Monash University, Melbourne, Australia
[2]Monash Institute of Railway Technology (IRT), Monash University, Melbourne, Australia
[3]School of Civil Engineering and Built Environment, Liverpool John Moores University, United Kingdom

Abstract

This study presents a validated three-dimensional finite element modelling framework for heavy axle load ballasted track, incorporating a resilient under ballast interlayer manufactured from reused end of life conveyor belt rubber, supporting circular-economy practice by diverting industrial rubber waste from landfill. The model is calibrated and validated against full-scale static and cyclic displacement measurements, then used to evaluate track response under static loading. Under static loading, the interlayer modifies support stiffness and redistributes load at the ballast-sub-ballast interface, reducing rail and sleeper deflections relative to track model without the resilient interlayer. Overall, the results indicate improved resilience while enabling sustainability-driven material reuse in heavy haul railway infrastructure.

Keywords: sustainable railway infrastructure, heavy axle load, finite element track model, end-of-life rubber, static and cyclic loading, resilient under-ballast interlayer.

1 Introduction

Heavy axle load (HAL) railway operations impose extreme stresses on ballasted track systems, accelerating ballast degradation and excessive track settlement, necessitating frequent maintenance interventions. High dynamic forces not only accelerate ballast degradation but also contribute to differential settlement, increased vibration transmission to the substructure, track stiffness irregularities, and progressive deterioration of track geometry quality, ultimately reducing the service life of the track system. To withstand high loads and efficiently transfer stresses to the substructure, HAL tracks are typically designed to be relatively stiff and constructed with heavier structural components, rails, and sleepers. However, stiffer track structure and uneven track stiffness result in increased dynamic loads, which accelerate rail wear and ballast degradation, ultimately reducing track stability. Furthermore, these issues are exacerbated by environmental factors, including waste generation from the track. This underlines the need for innovative solutions that improve track resilience while advancing environmental sustainability.

One approach to minimising dynamic forces and improving load transfer mechanisms in ballasted track structures is to optimise track stiffness and avoid large variations in it, particularly at transitions. The introduction of resilient components, such as Under Sleeper Pads (USPs) and Under-Ballast Mats (UBMs), can help manage stiffness transitions and improve track longevity. Previous studies have demonstrated that USPs and UBMs can mitigate dynamic amplification, improve stress distribution, and protect underlying structural layers [1, 2]. Sehner et al. [3] investigated the performance of UBMs in mitigating vibrations in heavy haul applications using measurements. Their results indicated a significant reduction in vibrations at specific frequencies following UBM installation. Several studies investigating the use of recycled rubber as a USP and UBM have reported increased interfacial contact areas at the sleeper-ballast and ballast-subballast interfaces, leading to reduced contact stresses and decreased ballast breakage [4, 5].

In parallel, sustainability considerations are driving the heavy haul rail industry to explore alternative solutions that incorporate recycled and reused materials, particularly those originating from the mining sector. Recycled elastomeric products, such as end-of-life (EOL) rubber conveyor belts (CBs), offer a potential source for developing sustainability-focused materials that also meet engineering performance requirements. End-of-life conveyor belts, together with off-the-road heavy-duty truck tyres, constitute a substantial industrial waste stream with significant potential to improve the mechanical properties of the track system [6]. Recent experimental and numerical studies have explored the feasibility of using EOL tyres as resilient layers in track structure, demonstrating positive effects on damping, stress attenuation, and vibration control [6, 7].

EOL-CBs are an underutilised resource with significant mechanical potential, yet they are often discarded in landfills or stockpiles. From an environmental standpoint, reusing and recycling EOL-CBs align with circular economy principles by reducing landfill waste, conserving natural resources, and lowering carbon emissions associated with the production of new materials, as illustrated in Figure 1. Economic benefits of using resilient components made from EOL-CBs include lower initial processing costs than those of other recycled materials or industrial competitors, and lower transportation costs when CBs are reused on-site in the heavy-haul mining industry. By addressing significant railway issues and promoting sustainability, this strategy offers a significant opportunity to enhance railway infrastructure performance and align with contemporary environmental and economic objectives.

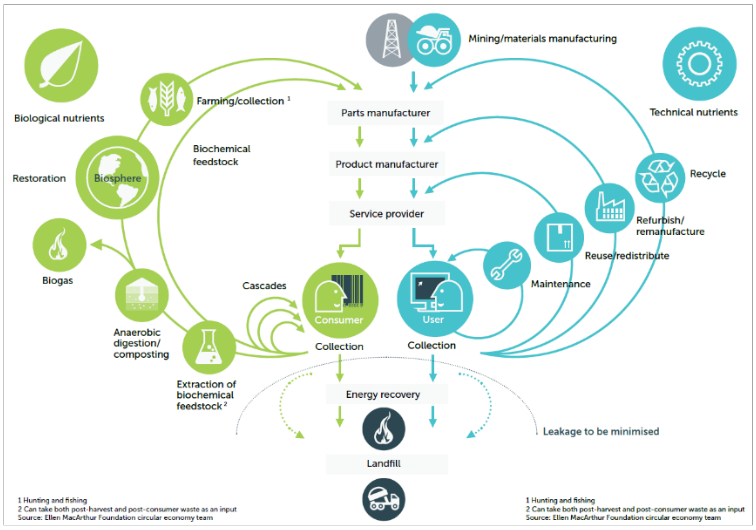

Figure 1: Concept diagram for a circular economy, including biological and technical cycles [8].

Experimental studies by Qi et al. [5] on track systems incorporating off-the-road truck tyres showed that such hybrid track layers can reduce ballast breakage and improve overall track stability. Although previous studies on the use of USPs and UBMs have shown performance improvements, these components are not yet widely used in HAL track systems. Moreover, the performance of resilient reused rubber components in heavy haul rail environments has not yet been investigated. Therefore, a better understanding of how resilient layers influence the dynamic response of the track assembly and the associated load transfer mechanisms under heavy haul loading is needed. The combined effects of heavy haul loading excitation, elastoplastic ballast behaviour, and recycled resilient materials necessitate advanced modelling and validation against experimental benchmarks. This paper summarises the advanced finite element (FE) track model, developed and validated against experimental data, which incorporates resilient layers and evaluates their impact on the structural performance of HAL track systems.

2 Methods

2.1 Numerical Model Development

A detailed three-sleeper three-dimensional finite element (FE) model of a ballasted track was developed in Abaqus, comprising the rail, sleepers, ballast, sub-ballast, and subgrade layers, as illustrated in Figure 2. The model configuration replicates the full-scale laboratory testing of ballasted track under phased static and cyclic loading reported by Čebašek et al. [9]. A comparable modelling framework was previously developed and calibrated using the same experimental data by Ramos et al. [10] to investigate the influence of track foundation stiffness on the performance of ballasted and slab track systems under similar loading conditions.

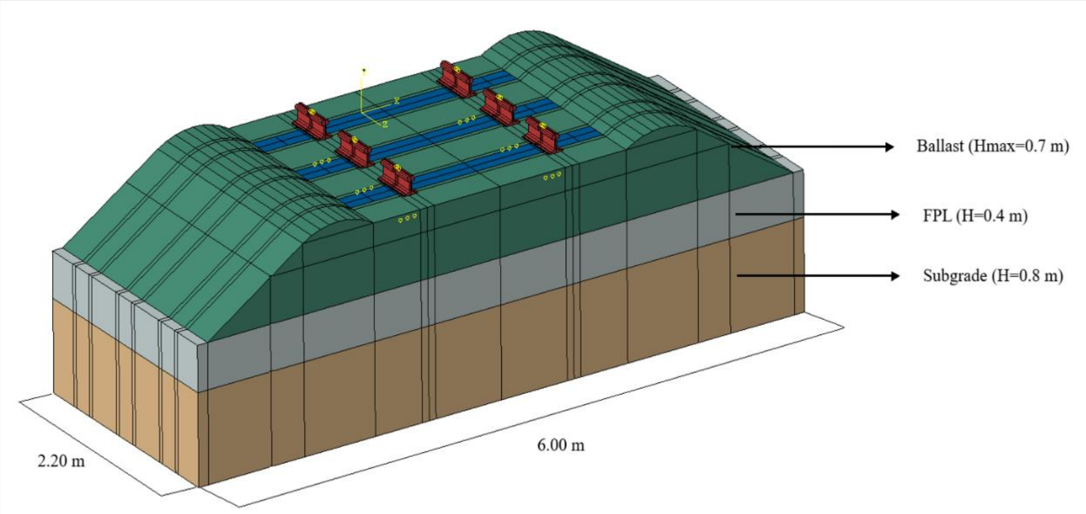

Figure 2: FE model layout developed.

Rails and sleepers were modelled as linear elastic solid elements. The rail cross-sectional geometry follows the BS113A(56E1) profile, while sleeper type G44 was modelled, as in the experimental program [9]. The properties of the sleeper are summarised in Table 1. The sleepers were spaced at 0.65 m centre to centre.

Material	**Constitutive model**	**Mass Density, ρ (kg/m3)**	**Elastic Modulus, E (MPa)**	**Poisson's Ratio, ν**	**Friction Angle, Ø**	**Dilation Angle, ψ**	**References**
Rail	Linear Elastic	7850	200,000	0.30	–	–	BS113A (56E1) [9]
Sleeper	Linear Elastic	2500	30,000	0.2	–	–	Sleeper G44 [9]
Ballast	Drucker-Prager	1600	110	0.30	40	5	[11]
Sub-ballast	Drucker-Prager	2220	$E = 1 \times Ev_2$ = 135	0.25	35	2	E is based on Ev_2 [9, 11]
Subgrade	Mohr-Coulomb	2220	$E = 1 \times Ev_2$ = 65	0.25	35	2	E is based on Ev_2 [9, 11]

Table 1: Mechanical properties of track components [9-11].

The ballast and sub-ballast layers were modelled as non-associated elastic–plastic materials governed by the three-dimensional Drucker–Prager (D–P) yield criterion, which is widely used for granular geomaterials. The adopted material properties for ballast and sub-ballast are listed in Table 1 and were selected based on published experimental and numerical studies [9, 10].

The subgrade layer was modelled as a linear elastic–perfectly plastic material governed by the Mohr–Coulomb failure criterion. The friction and dilation angles for the subgrade, sub-ballast, and ballast layers were selected based on representative values for hard limestone granular materials [9].

Contact interactions between adjacent layers were modelled using a “hard normal contact” to prevent penetration, with a tangential friction coefficient of 0.5. All components were discretised using 8-noded linear brick elements with reduced integration and hourglass control (C3D8R). Global element sizes of 0.05 m for the rail and 0.075 m for the remaining track components are assigned. Reduced integration leads to shorter analysis times by reducing the number of Gaussian integration points used to evaluate the integral. Appropriate mesh refinement was applied to ensure numerical accuracy, in accordance with validated modelling practices. Pinned boundary conditions were used on the base of the model, as shown in Figure 3, restricting translational displacements in the longitudinal (x), transverse (y), and vertical (z) directions. The x-y and y-z planes of the ballasted track were restricted from displacement in z and x directions, respectively.

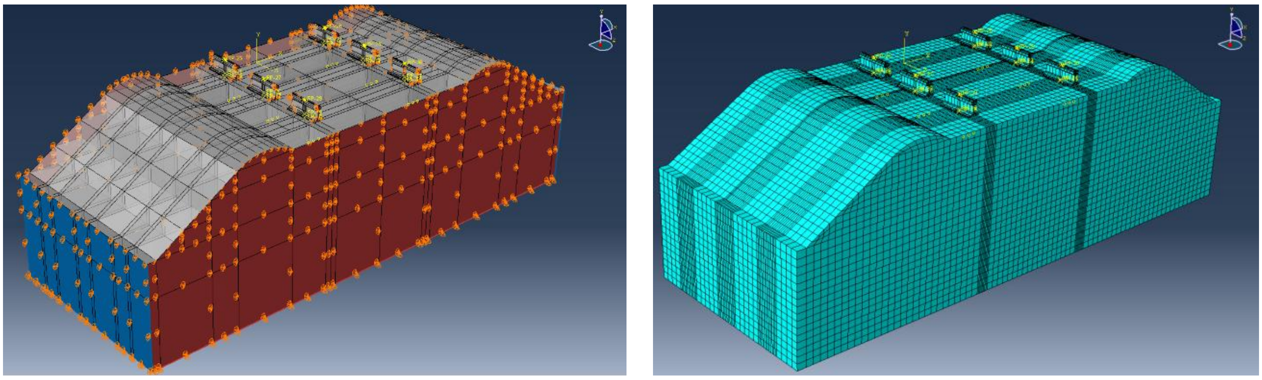

Figure 3: Left: applied boundary conditions; right: finite element mesh configuration used in the model.

Two resilient components were introduced in the track model assembly: a rail pad, between the rail seat and the sleeper, and UBM. The rail pads were modelled using an elastic–viscoelastic spring–dashpot representation to capture stiffness variations under static and dynamic loading. The rail pad (EPDM) was modelled as a spring with static stiffness of 22.5 MN/m and dynamic stiffness of 40 MN/m for cyclic simulations. For static and dynamic analyses, the dashpot coefficient was set to 10% of the corresponding spring stiffness, which were 2.25 MN·s/m and 4 MN·s/m, consistent with previous experimental studies [9].

UBMs, which have been represented as CBs, were modelled using a hyperelastic constitutive formulation. In compliance with ISO 7743, five uniaxial compression tests were conducted on 30 mm-thick, density 1095.65 kg/m^3 EOL steel cord conveyor belt (SC-CB) specimens, to characterise the conveyor belt material. Incompressible hyperelastic models were calibrated using the stress–strain data from the final stabilised loading cycle, as shown in Figure 4 in Abaqus. Similar material properties and thickness can be used in different thicknesses, as USP, which needs further studies. Ongoing laboratory testing is being conducted to further calibrate the mechanical properties of EOL fabric conveyor belts (F-CB) and EOL SC-CBs sourced from the Australian mining industry.

The Reduced Polynomial model with N-2 (R^2=0.9675), with C10 = 4.2056 × 10^5 Pa and C20 = 9.9298 × 10^5 Pa, was used in the Abaqus model based on the curve-fitting results.

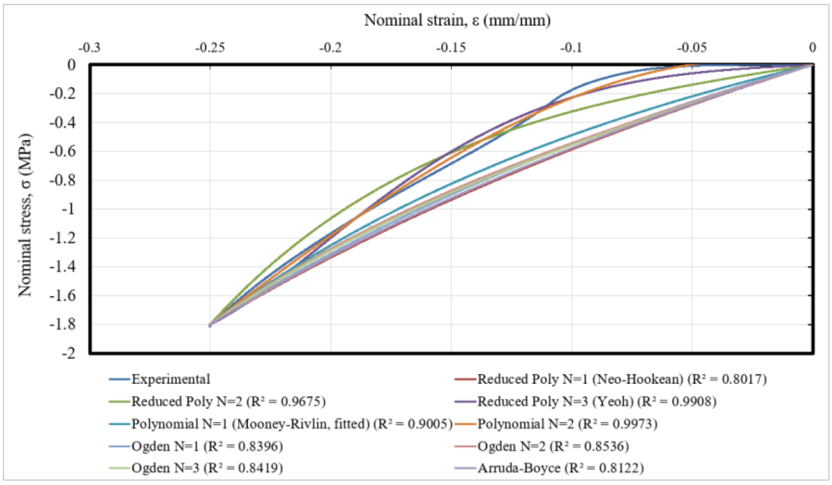

Figure 4: Uniaxial compression: experimental vs fitted hyperelastic models.

2.2 Loading Application

Both static and dynamic loads were applied, following the experimental approach of Cebasek et al. (2018) [9]. The static loading was applied in three steps. First, gravitational loading was applied for 200 s and maintained throughout the analysis. Second, a vertical load of 63.77 kN was applied to the middle sleeper over 620 s via three actuators, with redistributed loads of 15.94 kN, 31.88 kN, and 15.94 kN, respectively. The axle load applied to the central sleeper was taken as 63.77 kN. In the third step, the applied load was increased to 83.34 kN over 788 s, corresponding to loads of 20.84 kN, 41.69 kN, and 20.84 kN for the three actuators, respectively. During the static loading stage, the vertical axle load was set to 83.34 kN. This load distribution was modelled using a simplified load-sharing scheme in which the central sleeper carries approximately 50% of the applied vertical load, with the remaining 50% transferred symmetrically to the two adjacent sleepers, each carrying approximately 25%.

For the cyclic loading cases, the load distribution approach was not applied; instead, each sleeper was subjected to the full axle load, specified as 117.72 kN at 5.6 Hz and 166.71 kN at 2.5 Hz. The dynamic loading was applied in two stages. Gravity was applied for more than 1 s and maintained throughout the simulation. Subsequently, a cyclic vertical load ranging from 12 kN to 58.86 kN at 5.6 Hz and from 4 kN to 83.34 kN at 2.5 Hz was applied to each actuator (rail segment) using a periodic amplitude function over a total duration of 17.88 s to study the initial cycles. The time delay between adjacent sleepers was set to 0.0065 s at 5.6 Hz and 0.0144 s at 2.5 Hz, and the load redistribution among actuators was uniform.

2.3 Model Validation Procedure

The numerical model was calibrated and validated against full-scale experimental measurements obtained from laboratory testing of a ballasted track system conducted by Cebasek et al. [9]. The full-scale GRAFT-2 facility was used to assess the performance of ballasted track [9]. Loads were applied via six independent hydraulic actuators acting on full-size sleepers, while phased loading was used to simulate train passage, with each actuator loading a rail segment. Figure 5 shows the GRAFT-2 facility layout and key dimensions.

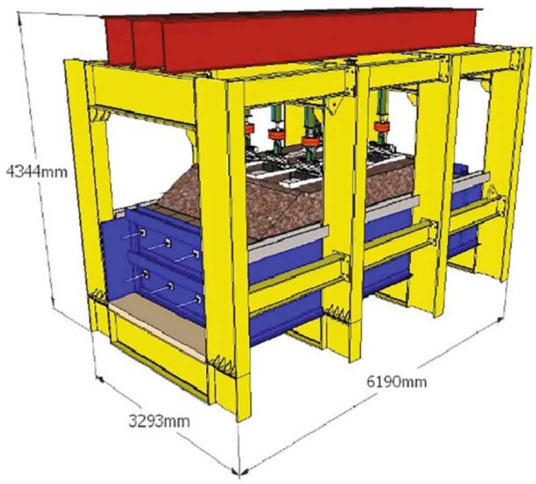

Figure 5: a) GRAFT-2 facility schematic and main geometric dimensions [9].

Model validation was performed by directly comparing numerical predictions with experimental measurements. Static and dynamic validation focused on rail and sleeper vertical displacements under incrementally applied load stages, as illustrated in Figure 6 and Figure 7. Overall, good agreement was achieved between numerical and experimental results. In static validation, the FE model slightly overestimated rail displacements and underestimated sleeper displacements, particularly at the highest load level (Step 3). These discrepancies can be attributed to uncertainties in the material properties assumption and contact conditions.

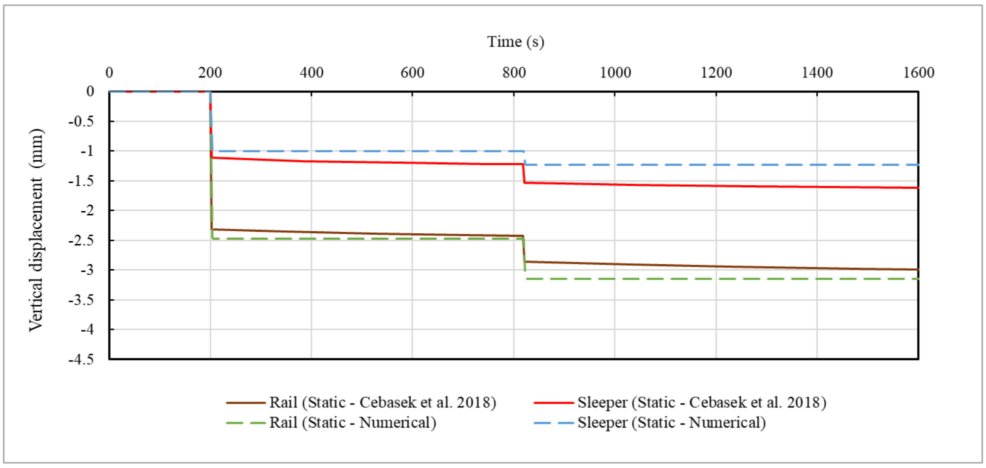

Figure 6*:* Comparison of numerical and experimental rail and sleeper displacements under static loading.

Dynamic validation was conducted by comparing numerical and experimental displacement responses of the rail and sleeper under cyclic loading at excitation frequencies of 2.5 Hz and 5.6 Hz. The midpoint of the cycle was taken as zero for convenience. The numerical model reproduced rail and sleeper displacement amplitudes with good accuracy at both frequencies. However, discrepancies were observed in rail and sleeper displacement responses, likely due to simplified ballast–sleeper interaction modelling and limitations in modelling the track stiffness variations among the three sleepers, and limitations of the model in capturing discrete particles rearrangement within the ballast layer under cyclic loading. After validation, the SC-CB layer was implemented in the numerical track model to investigate its influence on overall track behaviour.

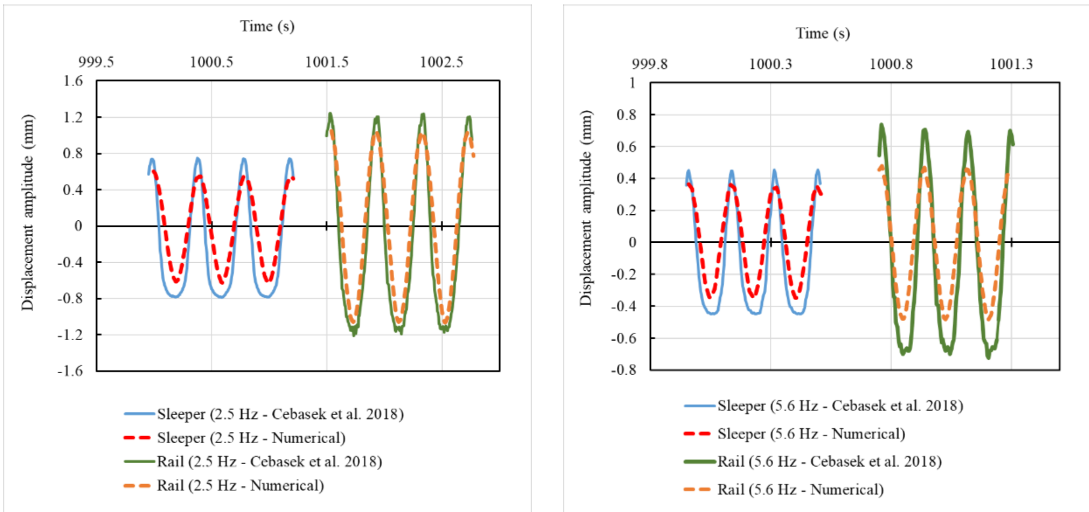

Figure 7*:* Model validation against the experimental results for dynamic displacement responses: (Left) rail and sleeper displacement at 2.5Hz; (Right) rail and sleeper displacement at 5.6 Hz [9].

3 Results

Following validation, a 30 mm thick SC-CB layer was incorporated beneath the ballast layer in the numerical track model (designated as CB-UBM in this study), as illustrated in Figure 8. For rubber components, a hybrid finite element formulation was employed to improve numerical stability and convergence, thereby enabling a more accurate representation of the nearly incompressible hyperelastic behaviour. To improve the accuracy of the stress-strain response and facilitate convergence of the nonlinear analyses, the mesh was locally refined in regions with strong stress gradients adjacent to CB.

After validating the vertical displacements at locations where LVDTs were implemented in an experimental test conducted by [9], the effect of CB-UBM on track performance was studied.

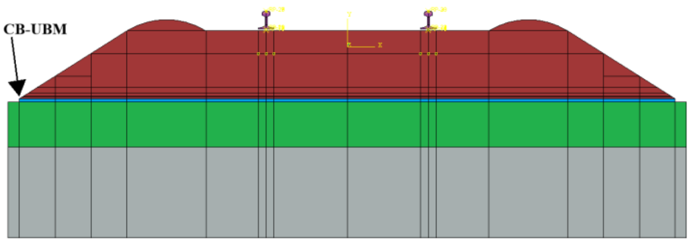

Figure 8: Geometry showing the location of CB-UBM below the ballast layer in the study.

3.1 CB-UBM Static Effect

Figure 9 demonstrates that incorporating the 30 mm CB-UBM leads to a consistent reduction in both rail and sleeper vertical displacements under static loading relative to the track model without the CB-UBM. With the CB UBM, the rail displacement decreased by 3% in the second step and by 2.97% in the third step, while the sleeper displacement decreased by 8.68% in the second step and by 8.84% in the third step. This behaviour is attributed to the resilient interlayer introduced between the ballast and sub-ballast.

The CB-UBM establishes a continuous interface that promotes a more uniform distribution of contact pressures across a wider area, thereby reducing peak stresses and limiting localised penetration of ballast into the sub ballast. As a result, the accumulated vertical deformation within the ballast and the upper sub-ballast is reduced, leading directly to smaller sleeper and rail deflections.

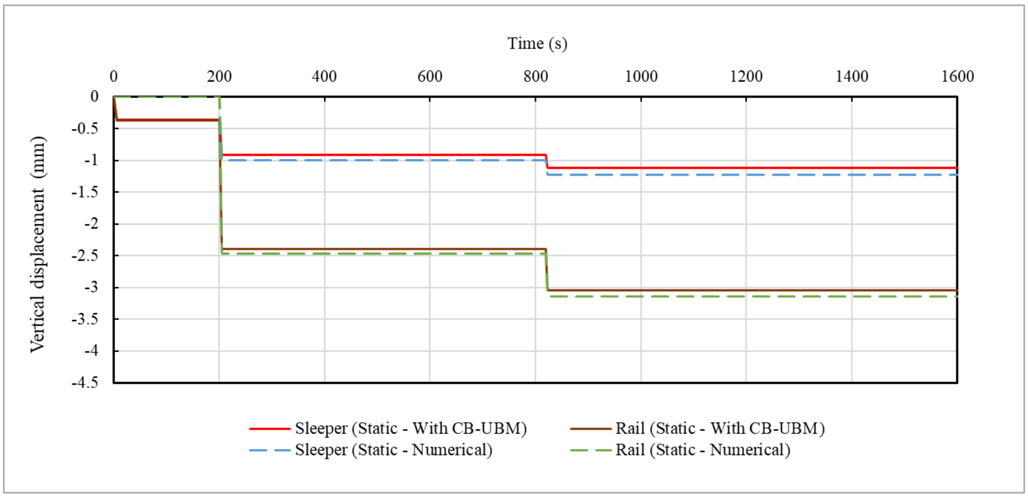

Figure 9: Comparison of rail and sleeper displacements under static loading for configurations with and without a 30 mm CB-UBM.

4 Conclusions and Contributions

This paper presents a validated numerical simulation framework for heavy axle-load tracks incorporating resilient UBMs, including sustainable alternatives derived from end-of-life conveyor-belt rubber. The model is calibrated and validated against experimental displacement. Preliminary simulation results indicate that under static loading, the CB-UBM functioned as a resilient interlayer that mitigated the support response and reduced rail and sleeper deflections relative to the track model without the CB-UBM. In addition, the frequency-dependent (dynamic) response of the CB-UBM is currently under investigation to clarify its vibration-mitigation performance under cyclic loading. In parallel with these numerical outcomes, ongoing experimental programmes to quantify the characteristic properties of both fabric and steel-cord conveyor belts will enable a more comprehensive assessment and support the development of more robust design guidance for their use as resilient under-ballast inclusions. This work provides a knowledge foundation to support the use of EOL conveyor belts for sustainability-driven material reuse.

Acknowledgements

The authors gratefully acknowledge Monash University for financial support enabling this PhD research, and thank colleagues and technical staff for their assistance.

References

1. Johansson, A., et al., *Under sleeper pads—Influence on dynamic train–track interaction.* Wear, 2008. **265**(9-10): p. 1479–1487.

2. Kraśkiewicz, C., et al., *Experimental and numerical testing of prototypical under ballast mats (UBMs) produced from deconstructed tires–The effect of mat thickness.* Construction and Building Materials, 2023. **369**: p. 130559.
3. Sehner, M., et al., *Vibration mitigation: under-ballast mats in heavy-haul applications.* Practice periodical on structural design and construction, 2023. **28**(4): p. 05023004.
4. Qi, Y., et al., *Sustainable solutions for railway using recycled rubber.* Transportation Geotechnics, 2024. **46**: p. 101256.
5. Indraratna, B., Q. Sun, and J. Grant, *Behaviour of subballast reinforced with used tyre and potential application in rail tracks.* Transportation Geotechnics, 2017. **12**: p. 26–36.
6. Indraratna, B., et al., *Sustainable performance of recycled rubber and mining waste utilized for efficient rail infrastructure.* Indian Geotechnical Journal, 2024. **54**(5): p. 1738–1750.
7. Ngo, T.N., B. Indraratna, and C. Rujikiatkamjorn, *Improved performance of ballasted tracks under impact loading by recycled rubber mats.* Transportation Geotechnics, 2019. **20**: p. 100239.
8. Tyre Stewardship Australia, L., E.P. Urban, and C. Randall Environmental, *The business case for a circular economy for Australia's off-the-road tyres, conveyors, and tracks*. 2023, Tyre Stewardship Australia Ltd: Australia.
9. Čebašek, T.M., et al., *Full scale laboratory testing of ballast and concrete slab tracks under phased cyclic loading.* Transportation Geotechnics, 2018. **17**: p. 33–40.
10. Ramos, A., et al., *Influence of track foundation on the performance of ballast and concrete slab tracks under cyclic loading: Physical modelling and numerical model calibration.* Construction and Building Materials, 2021. **277**: p. 122245.
11. Farooq, M.A., S. Nimbalkar, and B. Fatahi, *Three-dimensional finite element analyses of tyre derived aggregates in ballasted and ballastless tracks.* Computers and Geotechnics, 2021. **136**: p. 104220.
12. Barbero, E.J., *Finite element analysis of composite materials using Abaqus®.* 2023: CRC press.
13. Arema, L., *American railway engineering and maintenance-of-way association.* Manual for railway engineering, 2013. **2**: p. 55–57.